

---

# The Dilemma Between Dimensionality Reduction and Adversarial Robustness

---

**Sheila Alemany**

School of Computing & Information Sciences  
Florida International University  
Miami, FL  
salem010@fiu.edu

**Niki Pissinou**

School of Computing & Information Sciences  
Florida International University  
Miami, FL  
pissinou@fiu.edu

## Abstract

Recent work has shown the tremendous vulnerability to adversarial samples that are nearly indistinguishable from benign data but are improperly classified by the deep learning model. Some of the latest findings suggest the existence of adversarial attacks may be an inherent weakness of these models as a direct result of its sensitivity to well-generalizing features in high dimensional data. We hypothesize that data transformations can influence this vulnerability since a change in the data manifold directly determines the adversary’s ability to create these adversarial samples. To approach this problem, we study the effect of dimensionality reduction through the lens of adversarial robustness. This study raises awareness of the positive and negative impacts of five commonly used data transformation techniques on adversarial robustness. The evaluation shows how these techniques contribute to an overall increased vulnerability where accuracy is only improved when the dimensionality reduction technique approaches the data’s optimal intrinsic dimension. The conclusions drawn from this work contribute to understanding and creating more resistant learning models.

## 1 Introduction

There is a major concern on the immense fragility in neural networks when given a varying size set of adversarial samples, or imperceptibly perturbed inputs [Biggio and Roli, 2018, Su et al., 2019, Elsayed et al., 2018, Huang et al., 2017]. To address this issue, many pioneering works have risen to increase the models’ robustness or to maintain accurate prediction ability with the existence of these adversarial examples [Biggio and Roli, 2018, Ilyas et al., 2019, Elsayed et al., 2018, Hendrycks et al., 2019a, Goodfellow et al., 2018, Xu et al., 2017, Crecchi et al., 2019, Lee et al., 2019, Hendrycks et al., 2019b,c]. Previous work has proposed a variety of explanations for the intense vulnerability that these classifiers have to these imperceptibly perturbed inputs. Szegedy et al. [2013] initially argued the existence of low-probability adversarial “pockets” that an adversary can take advantage of during the creation of their samples. Goodfellow et al. [2014] made the connection between the ease of generating adversarial examples due to the linear nature of deep neural networks. Feinman et al. [2017] classified three cases where adversarial samples lie: (1) when the adversarial example is far away from the data manifold,<sup>1</sup> (2) when the submanifolds corresponding to different labels have pockets that allow the adversarial example to be on a submanifold of the wrong label further away from the classification boundary, and (3) when the adversarial example is near two submanifolds and close to the decision boundary. Most recently, Ilyas et al. [2019] argued that vulnerabilities arise due

---

<sup>1</sup>In mathematics, a data manifold is the geometry of the data which contains a topological space that locally resembles the Euclidean space near each data value. Each of these topological spaces per data value corresponds to an  $n$ -dimensional manifold with a neighborhood that is homeomorphic to the Euclidean space.

to a model’s well-generalizability of features in high dimensional data. However, the fundamental cause of the vulnerability has not been proven. As a result, the goal has been to disentangle the model to achieve robustness, either through standard regularization methods [Ilyas et al., 2019, Chun et al., 2020] or pre/post-processing of network input/outputs [Hendrycks et al., 2019a,c]. However, there is an ever-growing list of pre-processing techniques used in machine learning which are not used for increasing robustness [Tsai et al., 2019, Naranjo and Santos, 2019, Cohen et al., 2020, Aleman et al., 2018, Braten and Kraemer, 2018, Huang and Zhou, 2019, Alemany et al., 2019]. Since we hypothesize that any data transformation directly impacts the adversary’s ability to create adversarial samples due to manipulations in the data manifold, we focus on how five [Shlens, 2014, Golay and Kanevski, 2017, Bramer and Devedic, 2004, Chmielewski et al., 2015, Klinker, 2011] widely-used data transformation techniques affect the robustness of neural networks.

With this work, we introduce the positive and negative side effects that applying five frequently used dimensionality reduction techniques may have on a recurrent neural network given the Carlini & Wagner  $l_\infty$  [Carlini and Wagner, 2017a] evasion attack. To formally explain the difference in robustness, we propose that the inherent vulnerability does not solely stem from the ability of the neural network to generalize the features of high dimensionality data but also the increased capacity of the adversary to more efficiently<sup>2</sup> attack *as the dimensionality of the data strays from the optimal intrinsic dimension*. Lastly, evaluation results identify that the component-based dimensionality reduction technique, Principal Component Analysis (PCA), increases accuracy robustness by up to 24.39% only when reduced to the intrinsic dimension. Feature selection and trend extraction methods allow the adversary to employ more efficient evasion attacks for all evaluated perturbation budgets resulting in up to 65.85% increase in attack success. Additionally, we identify all five dimensionality reduction techniques reduce the precision robustness from 0.33 to at most 0.11 when the perturbation budget is above 0.68 with only PCA improving precision robustness from 0.48 to at most 0.84 when the perturbation budget is below 0.68.

## 2 Related Work

Adversarial machine learning has a considerable amount of prior work, so we focus on only the most related papers to our work in this section. Specifically, we briefly review previous works with defenses against adversarial attacks in the field of machine learning and, specifically, how dimensionality reduction has been used for robustness.

**Robustness** Due to the unknown fundamental and theoretical reasoning behind the immense vulnerability, various works attempt to reduce the impact of adversarial attacks, as in [Ilyas et al., 2019, Hendrycks et al., 2019a,c, Xu et al., 2017]. These techniques increase robustness by modifying the input such that the impact of gradient-based attacks are reduced, either through adversarial pre-training [Hendrycks et al., 2019a,c], feature squeezing [Xu et al., 2017], or identifying and removing the least “robust features” which contribute the most to a model’s vulnerability [Ilyas et al., 2019]. Unfortunately, adversarial attacks are still resilient. Ilyas et al. [2019] claimed that this is due to the theoretical foundational problem in machine learning which is built on the assumption that the training data accurately and adequately represents the underlying and *abstracted* phenomena through the learning process. As a result, given an adversarial sample, even with added robustness, the fundamental problem remains. Recent work has proposed that it is due to the high dimensionality<sup>3</sup> traditional abstraction techniques provide during training Mahloujifar et al. [2019], Crecchi et al. [2019], Shafahi et al. [2019], Ilyas et al. [2019].

**Dimensionality reduction** For decades, data dimensionality is often referred to as a “curse” due to the substantial computational complexity yielding difficulties when abstracting and understanding properties in data that do not occur in lower-dimensional data [Bingham and Mannila, 2001, Van Der Maaten et al., 2009]. Dimensionality reduction is the transformation of high-dimensional data into a significant representation of low dimensionality. As a result, it is not uncommon for dimensionality

---

<sup>2</sup>A more efficient attack consists of the adversary being able to induce inaccurate results using a "harder-to-detect" reduced perturbation budget.

<sup>3</sup>Highly dimensionality of a model is not only correlated to the model but also the dataset being used Su et al. [2019].

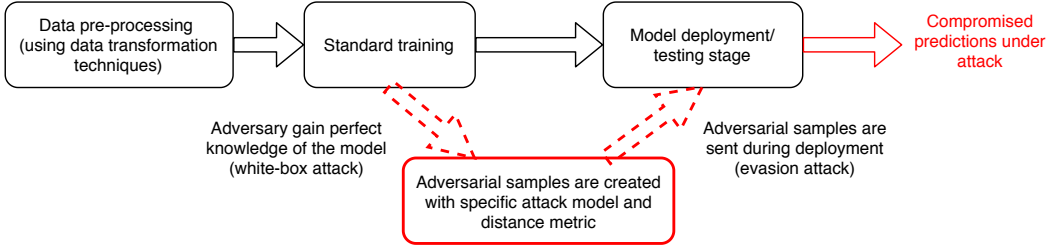


Figure 1: Machine learning pipeline in the presence of a white-box evasion adversarial attack. Data transformations are completed before the training stage; therefore, at the time of the attack, the adversary knows and uses the distribution of this processed data.

reduction techniques, such as Principle Component Analysis, to be used in various fields, such as data analytics or machine learning pre-processing, to improve upon these burdens [Cheng and Lu, 2018].

Dimensionality reduction has naturally influenced the field of adversarial machine learning due to the connection between adversarial vulnerability in deep learning and the high dimensionality of data. Xu et al. [2017] proposed feature squeezing for images in the input space that effectively forces the data to lie in a low dimensional manifold. Hendrycks and Gimpel [2016] and Crecchi et al. [2019] both proposed detection methods which take advantage of dimensionality reduction techniques as their primary defense component. Meanwhile, Bhagoji et al. [2018] and Bhagoji et al. [2017] proposed a defense that uses the component-based PCA and implies that incorporating PCA as pre-processing for the training data enhances the resilience of a fully-connected neural network. However, Carlini and Wagner [2017b] showed how the previously described techniques [Hendrycks and Gimpel, 2016, Bhagoji et al., 2017] were not consistent defenses. Against Bhagoji et al. [2017], they were able to show how using the dimensionality reduction technique, PCA, in the training data did not increase the robustness of a convolutional neural network, only the fully-connected network. Additionally, against Hendrycks and Gimpel [2016], they presented the argument that their proposed method only worked on the evaluated dataset MNIST due to the main difference between the adversarial and benign samples being the border-pixels since they are nearly always zero in the benign data. However, their defense was not effective when tested with another image dataset, CIFAR. Observing these inconsistencies, we hypothesize that widely-used linear data transformations such as component-based reduction, feature selection, and trend extraction techniques can negatively and directly impact the adversary’s ability to attack the model efficiently.

### 3 Learning Model

Generally, data pre-processing includes processes such as data cleaning, normalization, transformation, feature extraction, selection, and is the step done before training [Kotsiantis et al., 2006]. Figure 1 shows the machine learning pipeline considered in this work. In the following subsections, we formally describe the model used for training and the data transformation techniques evaluated in this work. Note that we did not implement any defenses as our goal for this work is to explore the impact of these techniques for small perturbation budgets that are difficult to detect using the current state-of-the-art defenses [Tjeng et al., 2019]. Considering the attack success rate with incorporated defenses and data transformation techniques is left for future work.

#### 3.1 Standard Training

We study multi-class classification, where input-label pairs  $(x, l) \in X \times \mathbb{Z}^+$  are sampled from a distribution  $D$  given a dataset, or input space,  $X$ . We model data in a high-dimensional space with embedded class-specific low-dimensional manifolds. Each training point (or input-label pair) belongs to one of  $N$  different classes. The classifier’s goal is to predict the class to which, given a new data point  $x$ , it will correctly predict the class  $l$  to which the new point belongs. Specifically, the class  $l$  is selected using the softmax function on the output of the model. More formally, the classifier’s objective is to learn  $C : X \rightarrow \mathbb{Z}^+$ , or in other words, predicting  $l \in L \subset \mathbb{Z}^+$  given a value  $x \in X$  where  $|L| = N$ .

There are various features mapping from the input space,  $X$ , each of these features are real numbers such that the features,  $\mathcal{F} = \{f : X \rightarrow \mathbb{R}\}$ . The feature values are normalized to (1) make the definitions throughout the models (including the attack models) scale-invariant and, (2) to aid in the learning process [Ilyas et al., 2019, Alemany et al., 2019]. Standard training occurs by performing minimization on a loss function  $L_\theta(x, l)$  over the input-label pairs  $(x, l)$  from the training set. With this work, we aim to explore a variety of linear data transformation techniques which affect the risk,  $\mathbb{E}_{(x, l) \sim D}[L_\theta(x, l)]$ . Just recently, this risk has been shown to have robustness bounds based the intrinsic<sup>4</sup> properties on the underlying data distribution  $D$  [Zhang et al., 2020]. Additionally, codimension<sup>5</sup> has been defined to strongly contribute to the pervasiveness of adversarial examples with no relation to the intrinsic properties of data [Khoury and Hadfield-Menell, 2018]. We specifically focus on the minimization of the codimension by aiming for the intrinsic dimensionality of data as the input  $(x, l)$  and its impact on the model robustness.

### 3.2 Data Transformation Techniques

Dimensionality reduction transforms a dataset  $X$  with dimensionality  $d$  to a new dataset  $X'$  with dimensionality  $d'$  such that the geometry of the data is maintained as much as possible. However, this is under the assumption that the geometry of the data manifold, or the intrinsic dimensionality  $d_i$  of the dataset  $X$ , is known. Such manifold is generally twisted and curved with non-uniformly distributed points on it, making the identification of the intrinsic dimensionality a challenging task specific to each individual dataset [Facco et al., 2017]. Therefore, dimensionality reduction is solved by assuming certain properties of the data in practice, such as the intrinsic dimension based on the variance of  $X$ . In this section, we describe and their potential impacts on a data manifold with the resulting robustness impacts in Section 5.

Note that our comparative review includes frequently used component-based reduction, feature selection, and trend extraction transformation techniques for data transformations, it is *not* exhaustive. We have strictly focused on widely-used linear data transformation techniques and their impact on the intrinsic dimension of data. Future work can be focused on non-linear dimensionality reduction techniques. We keep both works separate as we hypothesize that non-linear transformations impact the complexity of data manifolds in different ways than linear ones.

**Component-based reduction** Principal component analysis (PCA) is by far one of the more popular unsupervised tools due to its simple, non-parametric method for extracting relevant information from overwhelming datasets [Shlens, 2014]. PCA performs dimensionality reduction by embedding the data into a linear subspace of lower dimensionality by maximizing the amount of variance in the model [Van Der Maaten et al., 2009]. In other words, it constructs a low-dimensional representation of the data that describes as much of the variance in the data as possible, considering that the most variant features are the ones that contain the most information. For brevity, we assume the reader understands the mathematical background of PCA. For this work, we consider using 27%, 50%, and 81% of the principal components to approximate the feature counts around the 25, 50, and 75 quartiles. We explore how the selected  $p$  in varying extremes can significantly change the data manifold in diverse ways which impact robustness.

**Feature selection** Feature selection is a data transformation technique that has been used for decades to represent particular relationships in data by eliminating features that may be irrelevant or redundant [Dash and Liu, 1997]. These dimensionality reduction techniques select a subset of features where the original class distribution is still approximated based on a varying set size of heuristics used by different feature selection techniques. For this work, we have selected random forest selection [Golay and Kanevski, 2017] and low variance selection [Bramer and Devedic, 2004] due to their high usage for their low computational requirements.

Random forest selection has been shown to provide multivariate feature importance scores that are relatively cheap to obtain and have successfully been applied to high dimensional data [Menze et al., 2009]. This technique is an ensemble learner based on randomized decision trees and utilizes a

---

<sup>4</sup>The intrinsic dimensionality of data is the minimum number of parameters need to account for the observed properties in the data [Van Der Maaten et al., 2009].

<sup>5</sup>Codimension is the difference between the dimension of the data manifold and the dimension of the embedding space [Khoury and Hadfield-Menell, 2018].

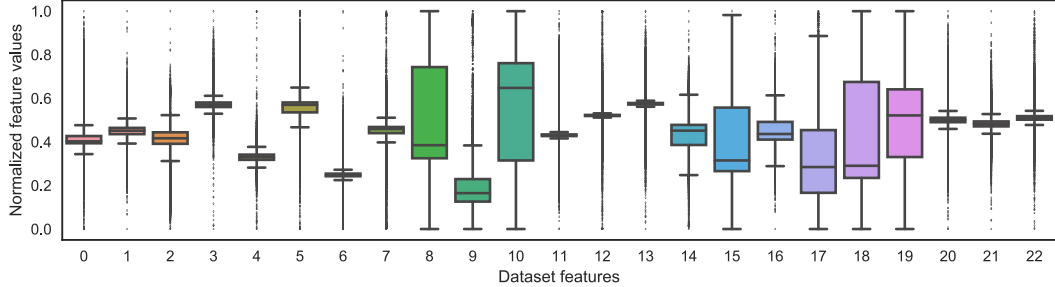


Figure 2: Boxplots to show the distribution of each feature from the MHealth (Mobile Health) Dataset [Banos et al., 2015]. We can see 9 of the 22 of the features contribute most of the variance in the data indicated by the height of each feature plot (approximately 84.8% of the total variance). More details regarding the dataset are described in Section 5.1.

feature importance measure, known as the “Gini importance” [Golay and Kanevski, 2017]. The features are selected if their importance measure is above a specified threshold. For this work, we set the threshold to be the mean of all importance values, as it is standard in practice [Pedregosa et al., 2011]. Low variance selection is a simple baseline approach to feature selection which removes all features whose variance do not meet a specified threshold [Bramer and Devedic, 2004]. This technique maximizes the variance in the model similar to PCA, however, there is no mapping onto a lower dimensional space. Additionally, since the variance of each feature is calculated independently, the relationship of features with the target variable is not considered in this feature selection technique unlike random forest selection.

For this work, we selected the features that contributed 91.1% of the variance in the data, resulting in a total of 11 features, as it is said to be the best heuristic to approximate the intrinsic dimension of a dataset [Van Der Maaten et al., 2009]. Both of the feature selection techniques chose 9 overlapping techniques and aligns with expectations since 9 features contributed most of the relevant information, as shown in Figure 2. As a result, we expect their impact on data manifolds to be similar even with their varying heuristics for feature selection.

**Trend extraction** Up-to-date works have focused on image recognition tasks concerning robustness, but time series data is also highly used in machine learning applications. As a result, we have analyzed the impact of data transformation techniques meant to extract trends in time series data, such as candlesticks [Chmielewski et al., 2015] and exponential moving average [Klinker, 2011]. These trend extraction techniques were selected as they are used in prediction tasks in areas such as the economics/financial markets [Naranjo and Santos, 2019, Cohen et al., 2020], the Internet of Things [Aleman et al., 2018, Braten and Kraemer, 2018], and object tracking [Huang and Zhou, 2019]. Although not typical dimensionality reduction techniques, we argue that these techniques affect the data manifold by smoothing the trends, similarly to feature squeezing for image recognition [Xu et al., 2017]. These trend extraction techniques do so by artificially reducing the distance between temporally adjacent points that provide better estimation of their distance along the manifold [Rahimi et al., 2007].

Candlestick data transformation converts each feature in  $\mathcal{F}$  into a series of candlesticks. A single candlesticks is a four-tuple containing the first value, last value, maximum, and minimum values a time window of the time series data – referred to as the open, close, high, and low values, respectively [Chmielewski et al., 2015]. The time window is defined from time  $t$  to time  $t + c$  with a consecutive candlestick starting at time  $t + c + 1$ , and so on. All the candlesticks have an equally sized time window of size  $c$ . The values in a candlestick are normalized as in [Chmielewski et al., 2015]. Once the dataset  $X$  of dimension  $d \times n$  gets transformed to  $X'$  of dimension  $4d \times \frac{n}{c}$ . The overall dimensionality of  $X$  is then only reduced if  $c \geq 4$ . For our evaluation, we only consider the case where the dimensionality is reduced. Exponential moving average (EMA) creates a series of averages of different subsets for each feature in  $\mathcal{F}$ . The EMA for a particular time  $t$  is calculated as  $x'(t) = \alpha x(t) + (1 - \alpha)x'(t - 1)$  where  $x'(t)$  and  $x(t)$  are the new EMA and original values at time  $t$  for a particular feature in  $\mathcal{F}$ , and  $\alpha$  is a smoothing factor in  $(0, 1]$  [Klinker, 2011]. This smoothing factor is calculated as  $\alpha = \frac{2}{c+1}$  where  $c$  is the assigned time window as previously described. In this case, the dimensionality of the

data is not necessarily reduced, however, the trends are extracted for a smoother manifold resulting in  $X$  effectively forced to lie in a lower dimensional manifold [Xu et al., 2017].

For this work, to ensure we are similarly comparing both trend extraction techniques, both were assigned the same value of  $c = 20$  for the time window. This value was a selected hyperparameter that would not reduce the dimensionality of the dataset enough to hinder the model accuracy for the candlestick technique but would cause a significant change to the feature trends given the EMA technique.

## 4 Threat Model

As per Carlini et al. [2019], in this section we define the adversary’s knowledge, capabilities, and goals to ensure analysis for worst-case robustness. Adversarial examples can be present in white-box and black-box threat models. In this paper, we use a white-box attack where the adversary has full access to the trained neural network model, the defense used, along with the data distribution at test time [Athalye et al., 2018]. We consider this attack because white-box attacks are more powerful than black-box attacks, as a white-box attack can reach a 100% success rate. Additionally, we consider evasion attacks where the adversaries can attack only during model deployment, meaning that they can only tamper with the input data after the deep learning model is trained. We utilize evasion attacks rather than poisoning attacks in this work because, even though poisoning attacks are effective, they require that the attacker access training data while being used to train a victim model. This assumption is often unrealistic, so poisoning attacks are not too severe against machine learning applications [Kwon et al., 2018].

**Adversarial Examples** Given a data point  $x$  and a classifier  $C$ , an adversarial sample  $x'$  satisfies two properties: (1)  $D(x, x') < \epsilon$  for some distance metric  $D$ , and (2)  $C(x) \neq C(x')$  [Athalye et al., 2018]. In other words, an adversarial input would be one such that  $x$  is perturbed with a budget lower than some small  $\epsilon$  such that it is classified incorrectly. Since it is not misclassified to some specific  $y'$ , simply any class as long as it is not the correct label  $y$ , this is known as an untargeted attack. Although targeted attacks are more powerful concerning the attack success rate, we are considering an untargeted attack since these attacks are more efficient (i.e., require a more limited perturbation budget) [Kwon et al., 2018, Carlini and Wagner, 2017a]. This smaller perturbation budget allows for an adversary to efficiently deploy the attack undetected [Carlini and Wagner, 2017a]. Therefore, it is more beneficial to understand how these dimensionality reduction techniques impact a model’s performance with harder to detect perturbations. For this work, we consider  $0 < \epsilon \leq 1.0$  [Tjeng et al., 2019].

In this paper, we use the  $l_\infty$  distortion metric to measure the similarity between  $x$  and  $x'$  since the  $l_\infty$ -ball around  $x$  has recently been studied as an optimal, natural notion for adversarial perturbations [Goodfellow et al., 2014, Carlini and Wagner, 2017a]. The  $l_\infty$  distance is defined as  $l_\infty = \|x - x'\|_\infty = \max(|x_1 - x'_1|, \dots, |x_n - x'_n|)$ . We can visualize the perturbation under this distance metric by viewing a series of data points. There is a maximum perturbation budget of  $\epsilon$ , where each value is allowed to be changed by up to  $\epsilon$ , with no limit on the number of modified values. Since  $D(x, x')$  has to remain less than some small  $\epsilon$ , even if all values are modified, the trends will appear visually identical.

**Attack Method** We generate adversarial samples using the iterative optimization-based method of Carlini and Wagner [2017a]. The goal of the attack is to find some value  $\gamma$  by minimizing  $D(x, x + \gamma) + c \cdot f(x + \gamma)$  such that  $x + \gamma \in [0, 1]^n$  where  $D$  is the distance metric described above,  $x$  is the input to be perturbed,  $f$  is an objective function such that  $C(x + \gamma) \neq y$ , and  $c$  is a constant value. To construct the samples, it completes 10,000 iterations of gradient descent with the Adam optimizer for each of the 20 carefully chosen values of  $c$ . We selected this attack model due to its high success at crafting effective adversarial samples with low distortion [Carlini and Wagner, 2017a, Zantedeschi et al., 2017]. Specifically, we have used the Carlini & Wagner  $l_\infty$  implementation from the Adversarial Robustness Toolbox by IBM Research [Nicolae et al., 2018].

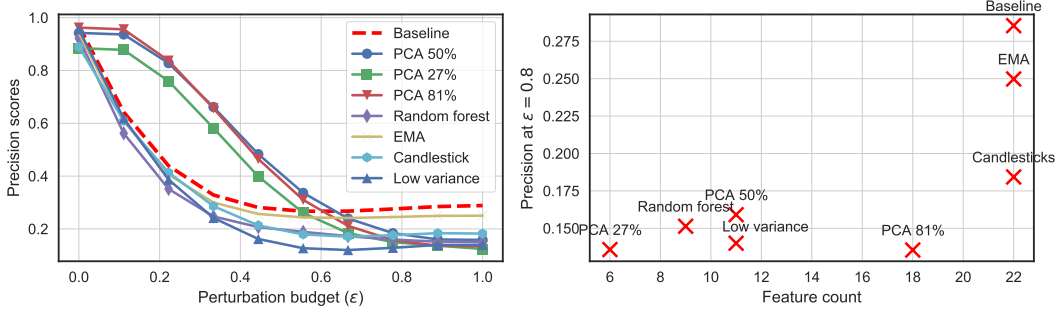


Figure 3: Precision scores under-performed for all techniques once the perturbation budget was over  $\epsilon = 0.68$ . From the scatter plot, we can see that reducing the number of features during training negatively impacted the precision scores given a high enough perturbation budget.

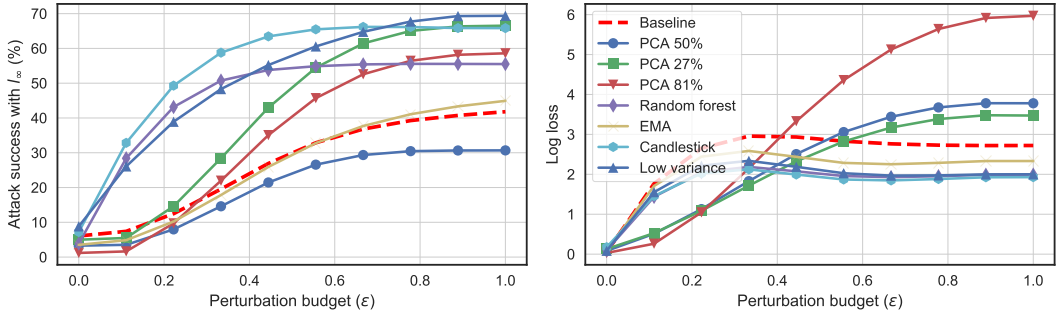


Figure 4: Attack success and log loss scores given five data transformation techniques against the baseline model without pre-processing. We can see that the best performing technique was PCA using half of the principal components. However, the log loss scores corresponding to model confident shows all PCA techniques returned the lowest confidence when  $\epsilon > 0.57$ .

## 5 Evaluating Robustness Against Evasion Attacks

### 5.1 Dataset and Model Setup

Recent state-of-the-art works are focused on image recognition tasks which results in evaluations being done on the same datasets, MNIST and CIFAR, most of the time. However, as described in Section 3.2, there are many high dimensional spaces in time series data that have received little attention in the adversarial machine learning field. Therefore, the need for evaluation on other datasets is crucial for the advancement of the area [Carlini and Wagner, 2017b]. As a result, for this work, we have used the MHealth (Mobile Health) Dataset<sup>6</sup> which contains body motion and vital signs recording of individuals while performing several physical activities [Banos et al., 2015]. This highly volatile dataset contains 22 total features which map to one of 12 potential physical activities and we selected the data corresponding to subject1 with a total of 160,860 rows, or values of  $x$ . For the classifier  $C$  described in Section 3.1, we have implemented a recurrent neural network with LSTM layers. Network architecture and hyperparameter tuning were completed to guarantee that all trained models received the same hyperparameters while maintaining testing accuracy above 90% to ensure that robustness results were not impacted by the network architecture. Further details regarding the data when compared against MNIST and CIFAR-10 can be found in Appendix B. The network architecture and implementation details are provided in Appendix A.

### 5.2 Discussion

Feinman et al. [2017] established that adversarial samples lie furthest away from the data manifold, and Goodfellow et al. [2014] established that adversarial perturbations on a sample  $x$  are created

<sup>6</sup>Dataset available on the UCI Machine Learning Repository at <https://archive.ics.uci.edu/ml/datasets/MHEALTH+Dataset>

as a gradient-based optimization problem. We also know that at the time of training, the weights correspond to a decision axis which captures an optimal boundary between the data manifolds and adversarial perturbations are restricted in the direction normal to the data manifold [Khoury and Hadfield-Menell, 2018]. From evaluation of the dataset, the intrinsic dimension  $d_i$  is approximated to be around 9 features of the 22 features based on the variance of the model [Van Der Maaten et al., 2009]. These are the main facts that we build on for our discussion.

**Manifold Impacts on Confidence and Precision** From Figure 3, we can see that precision is consistently below baseline for both feature selection and trend extraction techniques. The low log loss and precision indicates that these models are overly confident but erroneous due to the closer proximity between submanifolds to the decision axis. However, with PCA the precision is improved when  $\epsilon < 0.65$  due to better defined submanifolds as a direct result of mapping the input embedding into a lower dimension. The reduced precision is then introduced when the log loss of the model increases because linear units can get low precision from responding too strongly from a reduced confidence when it does not understand samples with larger perturbations [Goodfellow et al., 2014].

**Manifold Impacts on Accuracy** From Figure 4, it is clear the attack success rate is only hindered by 24.39% when the PCA technique is used with half of its principal components. Bhagoji et al. [2018] proposed that PCA should increase robustness because PCA removing the high variance components should eliminate the features that adversaries can easily take advantage of. However, as Carlini and Wagner [2017b], already showed this is not consistent given a convolutional neural network and it seems it is also not consistent with our recurrent neural network. This is only consistent in the case when the input embedding dimensionality approaches the intrinsic dimensionality. Given the intrinsic dimensionality reached with PCA 50%, the codimension is minimized resulting in the most restricted number of directions for the adversary to take advantage.

The other PCA techniques using 27% and 81% of the principal components did not perform as well once the perturbation budget exceeded  $\epsilon = 0.1$ . Particularly, using only 27% of the principal components results losing too many dimensions which can in turn reduce the manifold coverage for the dataset. The lack of coverage makes it is much easier for an adversary to find an example far away from the data manifold [Feinman et al., 2017]. This can happen easily in practice since high training/testing accuracy does not imply high accuracy/coverage of the data manifold [Khoury and Hadfield-Menell, 2018]. On the contrary, when using 81% of the principal components, there is high codimension resulting in relatively more directions normal to the manifold and directly contributing to a more efficient attack.

The feature selection techniques behaved similarly as expected given both techniques selected a majority of the same features. The lack of mapping to a lower dimension prevented the feature selection techniques to approximate the intrinsic dimension as well as PCA. In both cases, since no mapping occurs and a majority of the features are removed, the model contains high codimension and a lack of manifold coverage relative to the component-based techniques. As a result, feature selection allows for an efficient adversarial attack through all tested perturbation budgets. However, since random forest selection closer approximates the intrinsic dimension, the attack success rate differs to low variance selection by approximately 10%.

The trend extraction techniques, however, do not remove the features used but manage to force the data into a lower dimensional manifold. For the candlesticks, the transformation into the 4-tuple strayed the away from the intrinsic dimensionality by reshaping the features. This transformation contributed in fundamental information loss for the dataset while straying away from the intrinsic dimension resulting on the higher relative end of codimension and the one of most efficient creation of adversarial examples with a 60.98% decrease in robustness at  $\epsilon = 1.0$ . However, EMA seemed to not smooth the manifold enough for a drastic change from the baseline data. Therefore, no statistically significant change to the intrinsic dimension or the data manifold results in a performance on par with baseline. Table 1 shows a summary of the results.

## 6 Conclusion

For this work, we have shown the direct impacts that linear dimensionality reduction techniques have on the creation of adversarial samples and robustness of a model based on transformations to the data manifold. Overall, the component-based technique overperformed when the dimensionality

Table 1: Summary of results: Shows the number of features used from the original data, its clean accuracy when the model is not under attack, the perturbation budget required to attack success to 30%, and change in robustness at  $\epsilon = 0.80$  relative to the baseline model with no data transformation applied to its training data.

Data Transformation	Feature Count	Benign Accuracy	Distance ( $l_\infty$ )	$\Delta$ in Robustness
Baseline	22	97.93%	0.51	-
PCA	11	96.71%	0.40	$\uparrow 24.39\%$
PCA	18	98.80%	0.76	$\downarrow 43.90\%$
PCA	6	95.00%	0.34	$\downarrow 60.98\%$
Random Forest	9	96.11%	0.13	$\downarrow 31.71\%$
Low Variance	11	91.32%	0.15	$\downarrow 65.85\%$
Candlesticks	22	92.78%	0.11	$\downarrow 60.98\%$
EMA	22	96.48%	0.51	$\downarrow 7.32\%$

approached the intrinsic dimension. Although this number of principal components was not the identified intrinsic dimension, the direct mapping onto a lower dimension still allowed for a closer approximation when compared to the feature selection techniques, such as random forest. Meanwhile, the trend extraction techniques that refrained from sufficiently reaching the intrinsic dimension showed to not only negatively impact the attack success but also the precision scores. Therefore, future learning models under attack would benefit from using component-based techniques instead of feature selection or trend extraction techniques only if they approximate the intrinsic dimension.

## Broader Impact

In our work, we have only considered a recurrent neural network with LSTM layers. However, we believe that the benefits presented by the intrinsic dimension can be extended to other network architectures due to adversarial samples’ known generalized properties against data manifolds [Feinman et al., 2017, Khoury and Hadfield-Menell, 2018] and the similar vulnerabilities throughout machine learning models [Goodfellow et al., 2014, Bhagoji et al., 2018]. We also considered linear data transformation techniques that are widely used in practice, not for robustness, to bring awareness to those creating models of the negative impact that some pre-processing steps can contribute to their model.

We have shown that an adversary’s ability to craft malicious samples can be positively and negatively affected by widely-used data transformations on the input data. Positive impacts by dimensionality reduction techniques are only presented where technique embeds the high-dimensional input space into a low-dimensional structure that approaches the intrinsic dimension of data. Ilyas et al. [2019] recently proposed that adversarial samples’ vulnerability is due to the well-generalizability of the features. However, as the dimension approaches the optimal intrinsic dimension, lower codimension and higher manifold coverage are resulting in a lesser need to generalize features. This conclusion can contribute to the understanding and creation of more resistant learning models.

## References

Battista Biggio and Fabio Roli. Wild patterns: Ten years after the rise of adversarial machine learning. *Pattern Recognition*, 84:317–331, 2018.

Jiawei Su, Danilo Vasconcellos Vargas, and Kouichi Sakurai. One pixel attack for fooling deep neural networks. *IEEE Transactions on Evolutionary Computation*, 2019.

Gamaleldin F Elsayed, Shreya Shankar, Brian Cheung, Nicolas Papernot, Alex Kurakin, Ian Goodfellow, and Jascha Sohl-Dickstein. Adversarial examples that fool both human and computer vision. *arXiv preprint arXiv:1802.08195*, 2018.

Sandy Huang, Nicolas Papernot, Ian Goodfellow, Yan Duan, and Pieter Abbeel. Adversarial attacks on neural network policies. *arXiv preprint arXiv:1702.02284*, 2017.

Andrew Ilyas, Shibani Santurkar, Dimitris Tsipras, Logan Engstrom, Brandon Tran, and Aleksander Madry. Adversarial examples are not bugs, they are features. *arXiv preprint arXiv:1905.02175*, 2019.

Dan Hendrycks, Norman Mu, Ekin D Cubuk, Barret Zoph, Justin Gilmer, and Balaji Lakshminarayanan. Augmix: A simple data processing method to improve robustness and uncertainty. *arXiv preprint arXiv:1912.02781*, 2019a.

Ian Goodfellow, Patrick McDaniel, and Nicolas Papernot. Making machine learning robust against adversarial inputs. *Communications of the ACM*, 61(7), 2018.

Weilin Xu, David Evans, and Yanjun Qi. Feature squeezing: Detecting adversarial examples in deep neural networks. *arXiv preprint arXiv:1704.01155*, 2017.

Francesco Crecchi, Davide Bacciu, and Battista Biggio. Detecting adversarial examples through nonlinear dimensionality reduction. *arXiv preprint arXiv:1904.13094*, 2019.

Guang-He Lee, Yang Yuan, Shiyu Chang, and Tommi S Jaakkola. A stratified approach to robustness for randomly smoothed classifiers. *arXiv preprint arXiv:1906.04948*, 2019.

Dan Hendrycks, Mantas Mazeika, Saurav Kadavath, and Dawn Song. Using self-supervised learning can improve model robustness and uncertainty. In *Advances in Neural Information Processing Systems*, pages 15637–15648, 2019b.

Dan Hendrycks, Kimin Lee, and Mantas Mazeika. Using pre-training can improve model robustness and uncertainty. *arXiv preprint arXiv:1901.09960*, 2019c.

Christian Szegedy, Wojciech Zaremba, Ilya Sutskever, Joan Bruna, Dumitru Erhan, Ian Goodfellow, and Rob Fergus. Intriguing properties of neural networks. *arXiv preprint arXiv:1312.6199*, 2013.

Ian J Goodfellow, Jonathon Shlens, and Christian Szegedy. Explaining and harnessing adversarial examples. *arXiv preprint arXiv:1412.6572*, 2014.

Reuben Feinman, Ryan R Curtin, Saurabh Shintre, and Andrew B Gardner. Detecting adversarial samples from artifacts. *arXiv preprint arXiv:1703.00410*, 2017.

Sanghyuk Chun, Seong Joon Oh, Sangdoo Yun, Dongyo Han, Junsuk Choe, and Youngjoon Yoo. An empirical evaluation on robustness and uncertainty of regularization methods. *arXiv preprint arXiv:2003.03879*, 2020.

Yun-Cheng Tsai, Jun-Hao Chen, and Chun-Chieh Wang. Encoding candlesticks as images for patterns classification using convolutional neural networks. *arXiv preprint arXiv:1901.05237*, 2019.

Rodrigo Naranjo and Matilde Santos. A fuzzy decision system for money investment in stock markets based on fuzzy candlesticks pattern recognition. *Expert Systems with Applications*, 133:34–48, 2019.

Gil Cohen et al. Best candlesticks pattern to trade stocks. *International Journal of Economics and Financial Issues*, 10(2):256–261, 2020.

Concepcion Sanchez Aleman, Niki Pissinou, Sheila Alemany, and Georges A Kamhoua. Using candlestick charting and dynamic time warping for data behavior modeling and trend prediction for mwsn in iot. In *2018 IEEE International Conference on Big Data (Big Data)*, pages 2884–2889. IEEE, 2018.

Anders Eivind Braten and Frank Alexander Kraemer. Towards cognitive iot: Autonomous prediction model selection for solar-powered nodes. In *2018 IEEE International Congress on Internet of Things (ICIOT)*, pages 118–125. IEEE, 2018.

Jianglei Huang and Wengang Zhou. Re 2 ema: Regularized and reinitialized exponential moving average for target model update in object tracking. In *Proceedings of the AAAI Conference on Artificial Intelligence*, volume 33, pages 8457–8464, 2019.

Sheila Alemany, Jonathan Beltran, Adrian Perez, and Sam Ganzfried. Predicting hurricane trajectories using a recurrent neural network. In *Proceedings of the AAAI Conference on Artificial Intelligence*, volume 33, pages 468–475, 2019.

Jonathon Shlens. A tutorial on principal component analysis. *arXiv preprint arXiv:1404.1100*, 2014.

Jean Golay and Mikhail Kanevski. Unsupervised feature selection based on the morisita estimator of intrinsic dimension. *Knowledge-Based Systems*, 135:125–134, 2017.

Max Bramer and Vladan Devedic. *Artificial Intelligence Applications and Innovations*. Springer, 2004.

Leszek Chmielewski, Maciej Janowicz, Joanna Kaleta, and Arkadiusz Orłowski. Pattern recognition in the japanese candlesticks. In *Soft computing in computer and information science*, pages 227–234. Springer, 2015.

Frank Klinker. Exponential moving average versus moving exponential average. *Mathematische Semesterberichte*, 58(1):97–107, 2011.

Nicholas Carlini and David Wagner. Towards evaluating the robustness of neural networks. In *2017 ieee symposium on security and privacy (sp)*, pages 39–57. IEEE, 2017a.

Saeed Mahloujifar, Dimitrios I Diochnos, and Mohammad Mahmoody. The curse of concentration in robust learning: Evasion and poisoning attacks from concentration of measure. In *Proceedings of the AAAI Conference on Artificial Intelligence*, volume 33, pages 4536–4543, 2019.

Ali Shafahi, W Ronny Huang, Christoph Studer, Soheil Feizi, and Tom Goldstein. Are adversarial examples inevitable? *International Conference on Learning Representations*, 2019.

Ella Bingham and Heikki Mannila. Random projection in dimensionality reduction: applications to image and text data. In *Proceedings of the seventh ACM SIGKDD international conference on Knowledge discovery and data mining*, pages 245–250, 2001.

Laurens Van Der Maaten, Eric Postma, and Jaap Van den Herik. Dimensionality reduction: a comparative. *J Mach Learn Res*, 10(66-71):13, 2009.

Zhun Cheng and Zhixiong Lu. A novel efficient feature dimensionality reduction method and its application in engineering. *Complexity*, 2018, 2018.

Dan Hendrycks and Kevin Gimpel. Early methods for detecting adversarial images. *arXiv preprint arXiv:1608.00530*, 2016.

Arjun Nitin Bhagoji, Daniel Cullina, Chawin Sitawarin, and Prateek Mittal. Enhancing robustness of machine learning systems via data transformations. In *2018 52nd Annual Conference on Information Sciences and Systems (CISS)*, pages 1–5. IEEE, 2018.

Arjun Nitin Bhagoji, Daniel Cullina, and Prateek Mittal. Dimensionality reduction as a defense against evasion attacks on machine learning classifiers. *arXiv preprint arXiv:1704.02654*, 2, 2017.

Nicholas Carlini and David Wagner. Adversarial examples are not easily detected: Bypassing ten detection methods. In *Proceedings of the 10th ACM Workshop on Artificial Intelligence and Security*, pages 3–14, 2017b.

SB Kotsiantis, Dimitris Kanellopoulos, and PE Pintelas. Data preprocessing for supervised learning. *International Journal of Computer Science*, 1(2):111–117, 2006.

Vincent Tjeng, Kai Xiao, and Russ Tedrake. Evaluating robustness of neural networks with mixed integer programming. *International Conference on Learning Representations*, 2019.

Xiao Zhang, Jinghui Chen, Quanquan Gu, and David Evans. Understanding the intrinsic robustness of image distributions using conditional generative models. *arXiv preprint arXiv:2003.00378*, 2020.

Marc Khouri and Dylan Hadfield-Menell. On the geometry of adversarial examples. *arXiv preprint arXiv:1811.00525*, 2018.

Elena Facco, Maria d'Errico, Alex Rodriguez, and Alessandro Laio. Estimating the intrinsic dimension of datasets by a minimal neighborhood information. *Scientific reports*, 7(1):1–8, 2017.

Oresti Banos, Jose Antonio Moral-Munoz, Ignacio Diaz-Reyes, Manuel Arroyo-Morales, Miguel Damas, Enrique Herrera-Viedma, Choong Seon Hong, Sungyong Lee, Hector Pomares, Ignacio Rojas, et al. mdurance: a novel mobile health system to support trunk endurance assessment. *Sensors*, 15(6):13159–13183, 2015.

Manoranjan Dash and Huan Liu. Feature selection for classification. *Intelligent data analysis*, 1(3):131–156, 1997.

Bjoern H Menze, B Michael Kelm, Ralf Masuch, Uwe Himmelreich, Peter Bachert, Wolfgang Petrich, and Fred A Hamprecht. A comparison of random forest and its gini importance with standard chemometric methods for the feature selection and classification of spectral data. *BMC bioinformatics*, 10(1):213, 2009.

F. Pedregosa, G. Varoquaux, A. Gramfort, V. Michel, B. Thirion, O. Grisel, M. Blondel, P. Prettenhofer, R. Weiss, V. Dubourg, J. Vanderplas, A. Passos, D. Cournapeau, M. Brucher, M. Perrot, and E. Duchesnay. Scikit-learn: Machine learning in Python. *Journal of Machine Learning Research*, 12:2825–2830, 2011.

Ali Rahimi, Ben Recht, and Trevor Darrell. Learning to transform time series with a few examples. *IEEE Transactions on Pattern Analysis and Machine Intelligence*, 29(10):1759–1775, 2007.

Nicholas Carlini, Anish Athalye, Nicolas Papernot, Wieland Brendel, Jonas Rauber, Dimitris Tsipras, Ian Goodfellow, Aleksander Madry, and Alexey Kurakin. On evaluating adversarial robustness. *arXiv preprint arXiv:1902.06705*, 2019.

Anish Athalye, Nicholas Carlini, and David Wagner. Obfuscated gradients give a false sense of security: Circumventing defenses to adversarial examples. *arXiv preprint arXiv:1802.00420*, 2018.

Hyun Kwon, Yongchul Kim, Ki-Woong Park, Hyunsoo Yoon, and Daeseon Choi. Friend-safe evasion attack: An adversarial example that is correctly recognized by a friendly classifier. *computers & security*, 78:380–397, 2018.

Valentina Zantedeschi, Maria-Irina Nicolae, and Ambrish Rawat. Efficient defenses against adversarial attacks. In *Proceedings of the 10th ACM Workshop on Artificial Intelligence and Security*, pages 39–49, 2017.

Maria-Irina Nicolae, Mathieu Sinn, Minh Ngoc Tran, Beat Bueser, Ambrish Rawat, Martin Wistuba, Valentina Zantedeschi, Nathalie Baracaldo, Bryant Chen, Heiko Ludwig, Ian Molloy, and Ben Edwards. Adversarial robustness toolbox v1.2.0. *CoRR*, 1807.01069, 2018. URL <https://arxiv.org/pdf/1807.01069.pdf>.

Andrej Karpathy, Justin Johnson, and Li Fei-Fei. Visualizing and understanding recurrent networks. *arXiv preprint arXiv:1506.02078*, 2015.

François Chollet et al. Keras. <https://github.com/fchollet/keras>, 2015.

Yann LeCun, Corinna Cortes, and CJ Burges. Mnist handwritten digit database. *ATT Labs [Online]. Available: http://yann.lecun.com/exdb/mnist*, 2, 2010.

Alex Krizhevsky. Learning multiple layers of features from tiny images. Technical report, 2009.

## A Network Architecture and Implementation Details

In this paper, we conducted the evaluation using a fully-connected recurrent neural network (RNN) used to explore the impact of the Carlini and Wagner  $l_\infty$  evasion attack on time series data. As previously described, hyperparameters were optimally selected before the training began through a grid search. These parameters were chosen to maintain the model accuracy of all models above 90% to ensure the selected parameters did not impact robustness results.

For the network architecture, five total layers were employed: an input layer, three hidden layers, and an output layer. The input layer takes as input a data tuple containing a sequence of features. This sequence is used for the RNN to learn over consecutive data values, maintaining the time-dependent relationship of the dataset. The sequence length used in this work was 100 for all models, except for the models with the trend extraction data transformation techniques with a sequence length of 5 due to their window size of 20. The output layer contains a dense layer with the final activation function, softmax. We used the softmax function to calculate the output probability vector  $y$  to guarantee that it satisfies  $\forall i \in N, 0 \leq y_i \leq 1$  and  $y_1 + y_2 + \dots + y_N = 1$  where  $N$  was the total number of possible feature labels. The hidden state vectors, or hidden layers, contain only two LSTM units combined with dropout layers as it has been shown that at least two hidden state vectors in RNNs return satisfactory results, and more than three do not provide significant improvement [Karpathy et al., 2015]. In these hidden vectors, we used the hyperbolic tangent function as it is the standard activation function among recurrent neural networks [Chollet et al., 2015], and the dropout values were set to 0.1 implying that 10% of each input was ignored in order to prevent the model from overfitting to the training data.

Overall, since our goal was to explore the vulnerabilities in RNNs that are frequently used in various applications, we kept our network architecture closer to the default models (provided by Keras [Chollet et al., 2015]) as possible as long as we maintained a high enough accuracy across all dimensionality reduction techniques. We are not concerned about the simple linear structure of our network as Carlini and Wagner [2017a] claimed their attacks are not impacted by the simple structure in the network architecture. Lastly, the attack hyperparameters used for the Carlini and Wagner  $l_\infty$  implementation from the Adversarial Robustness Toolbox by IBM Research [Nicolae et al., 2018] are shown in Table 2, as well. The models were all trained on an NVIDIA GeForce GTX 1060 with Max-Q Design.

Table 2: Model parameters for all data transformation techniques where all techniques reached a training accuracy of at least 90%.

Parameters	Standard Training	Adversarial Training
Confidence	-	0.5
Learning rate	0.001	0.01
Dropout	0.1	-
Batch size	512	512
Epochs	250	-

For the implementation, we utilized Keras [Chollet et al., 2015], the API that integrates the lower-level deep learning languages such as TensorFlow. Keras is used to facilitate the process of using deep learning models in practice and has been increasingly used in industry and the research community [Chollet et al., 2015]. We used the default learning rate hyperparameter of 0.001. The dataset used was divided where 85% of the data was used for training, and 15% was used for testing. Due to the various data transformation techniques, the specific shape of the data used for training and testing are depicted in Table 3.

## B Dataset Comparison Against MNIST and CIFAR-10

The focus of today’s adversarial evaluation is largely centered around image recognition tasks, specifically using the MNIST [LeCun et al., 2010] and CIFAR-10 [Krizhevsky, 2009] datasets. However, the time series data area contains various high dimensional datasets that have received little attention yet are highly used throughout applications, as described in Section 3 when discussing the

Table 3: Training and testing set dimensions used for evaluation with varying data transformation techniques. The sequence length is 5 for the trend extraction techniques due to the time window of size  $c = 20$ .

Data Transformation	Training shape ( $X$ )	Testing shape ( $X$ )
Baseline	(136646, 100, 22)	(24114, 100, 22)
PCA ( $p = 11$ )	(136646, 100, 11)	(24114, 100, 12)
PCA ( $p = 18$ )	(136646, 100, 18)	(24114, 100, 18)
PCA ( $p = 6$ )	(136646, 100, 6)	(24114, 100, 6)
Random Forest	(136646, 100, 9)	(24114, 100, 11)
Low Variance	(136646, 100, 11)	(24114, 100, 11)
Candlesticks	(6831, 5, 115)	(1206, 5, 115)
EMA	(136726, 5, 22)	(24129, 5, 22)

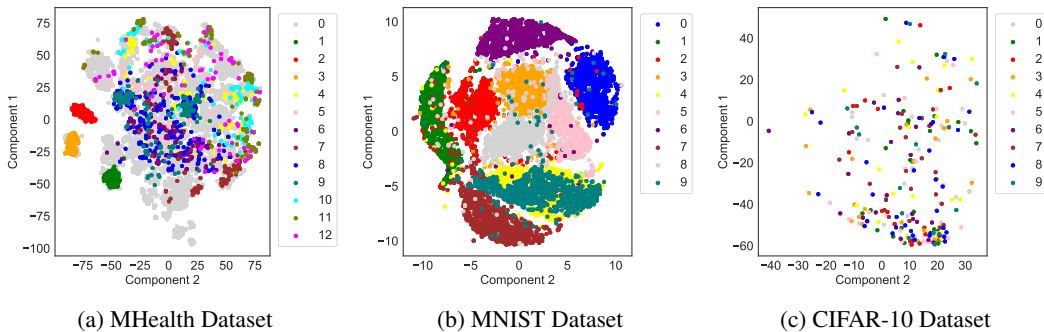


Figure 5: Visualization of datasets using T-SNE to observe the relationships between the points in high-dimensional space using 1000 randomly selected points from each dataset.

trend extraction techniques. As described in Section 5.1, for this work, we have used the MHealth (Mobile Health) Dataset for our time series evaluation.

From Figure 5b, we can see that the MNIST dataset contains the best well-defined classes where points corresponding to the same class are clustered together. This implies that the points within each class of the MNIST dataset have highly correlated relationships even with the highly-dimensional dataset. On the contrary, in Figure 5c, the CIFAR-10 dataset does not have well-defined clusters resulting an almost opposite conclusion relative to the MNIST dataset. As a result, CIFAR-10 has been described as a substantially more difficult dataset to work with and therefore, MNIST may contain properties that do not generalize across tougher datasets such as CIFAR-10 [Carlini and Wagner, 2017b].

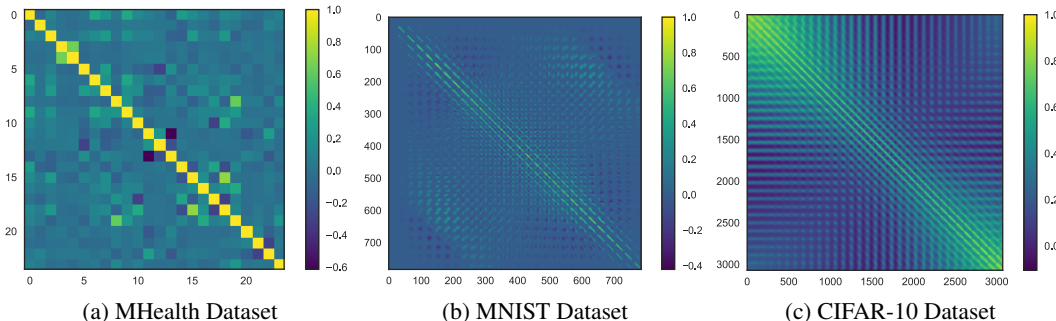


Figure 6: Pearson correlation similarities between features in each dataset. The average Pearson correlation values are 0.0697, 0.0192, and 0.2506 for MHealth, MNIST, and CIFAR-10, respectively.

The MHealth dataset, however, lies between the MNIST and CIFAR-10 dataset in regards to the relationship between the points in high-dimensional space. From the Figure 5a, we can see that there are various clusters that can be easily identified, such as the points in class 1, 2, and 3. Yet, there are cases such as with the points in class 8 and 12, where the points are more scattered. Additionally, from Figure 6, we can see that the MNIST dataset is also the most similar between individual features when compared against MHealth and the CIPHAR-10 datasets. As a result, we are evaluating with a medical data dataset that is not only a realistic real time series dataset, but also contains manifold properties that may carry-out to various other highly-dimensional time series datasets. As a result, we believe our evaluation on the MHealth dataset is sufficient for the concluding results in this work.